



DAG: A Dual Causal Network for Time Series Forecasting with Exogenous Variables

Xiangfei Qiu
East China Normal University
Shanghai, China
xfqiu@stu.ecnu.edu.cn

Yuhan Zhu
East China Normal University
Shanghai, China
yhzhu@stu.ecnu.edu.cn

Zhengyu Li
East China Normal University
Shanghai, China
lizhengyu@stu.ecnu.edu.cn

Hanyin Cheng
East China Normal University
Shanghai, China
hycheng@stu.ecnu.edu.cn

Xingjian Wu
East China Normal University
Shanghai, China
xjwu@stu.ecnu.edu.cn

Chenjuan Guo
East China Normal University
Shanghai, China
cjguo@dase.ecnu.edu.cn

Bin Yang
East China Normal University
Shanghai, China
byang@dase.ecnu.edu.cn

Jilin Hu ✉
East China Normal University
Shanghai, China
jlhu@dase.ecnu.edu.cn

Abstract

Time series forecasting is crucial in various fields such as economics, traffic, and AIOps. However, in real-world applications, focusing solely on the endogenous variables (i.e., target variables), is often insufficient to ensure accurate predictions. Considering exogenous variables (i.e., covariates) provides additional predictive information, thereby improving forecasting accuracy. However, existing methods for time series forecasting with exogenous variables (TSF-X) have the following shortcomings: 1) they do not leverage future exogenous variables, 2) they fail to account for the causal relationships between endogenous and exogenous variables. As a result, their performance is suboptimal. In this study, to better leverage exogenous variables, especially future exogenous variable, we propose a general framework **DAG**, which utilizes *Dual cAusal network along both the temporal and channel dimensions for time series forecasting with exoGenous variables*. Specifically, we first introduce the *Temporal Causal Module*, which includes a causal discovery module to capture how historical exogenous variables affect future exogenous variables. Following this, we construct a causal injection module that incorporates the discovered causal relationships into the process of forecasting future endogenous variables based on historical endogenous variables. Next, we propose the *Channel Causal Module*, which follows a similar design principle. It features a causal discovery module models how historical exogenous variables influence historical endogenous variables, and a causal injection module incorporates the discovered relationships to enhance the prediction

of future endogenous variables based on future exogenous variables. Extensive experiments on multiple datasets demonstrate the state-of-the-art performance of DAG. Additionally, all datasets and code are available at <https://github.com/decisionintelligence/DAG>.

Keywords

deep learning; time series forecasting; exogenous variables

ACM Reference Format:

Xiangfei Qiu, Yuhan Zhu, Zhengyu Li, Hanyin Cheng, Xingjian Wu, Chenjuan Guo, Bin Yang, and Jilin Hu ✉. 2025. DAG: A Dual Causal Network for Time Series Forecasting with Exogenous Variables. In *Proceedings of Make sure to enter the correct conference title from your rights confirmation email (Conference acronym 'XX)*. ACM, New York, NY, USA, 13 pages. <https://doi.org/10.1145/nnnnnnnn.nnnnnnnn>

1 Introduction

Time series forecasting plays a vital role in many real-world applications, including economic [15, 43, 47], traffic [27, 35, 49, 53, 63], health [20, 34, 51, 57], energy [1, 12], and AIOps [4, 18, 40, 44, 54, 61]. Given historical observations, it is valuable if we can know the future values ahead of time. With the rapid development of deep learning, numerous forecasting methods have been proposed [7, 28–30, 41, 60, 62], most of which focus on univariate or multivariate time series and rely on learning the temporal dependencies within a single endogenous (i.e., target) variable or across multiple endogenous variables—see Figure 1a.

However, in addition to the endogenous variables themselves, many practical scenarios involve another type of information that significantly influences the accuracy of predictions—exogenous variables (i.e., covariates). Particularly in scenarios where future exogenous variables are available, effectively leveraging such auxiliary information has the potential to greatly enhance forecasting performance. For example, in traffic prediction, having access to future weather conditions can improve the estimation of future traffic volume; in retail sales forecasting, incorporating holiday schedules and promotional campaigns can lead to better inventory

Permission to make digital or hard copies of all or part of this work for personal or classroom use is granted without fee provided that copies are not made or distributed for profit or commercial advantage and that copies bear this notice and the full citation on the first page. Copyrights for components of this work owned by others than the author(s) must be honored. Abstracting with credit is permitted. To copy otherwise, or republish, to post on servers or to redistribute to lists, requires prior specific permission and/or a fee. Request permissions from permissions@acm.org.
Conference acronym 'XX, June 03–05, 2018, Woodstock, NY

© 2025 Copyright held by the owner/author(s). Publication rights licensed to ACM.
ACM ISBN 978-1-4503-XXXX-X/2018/06
<https://doi.org/10.1145/nnnnnnnn.nnnnnnnn>

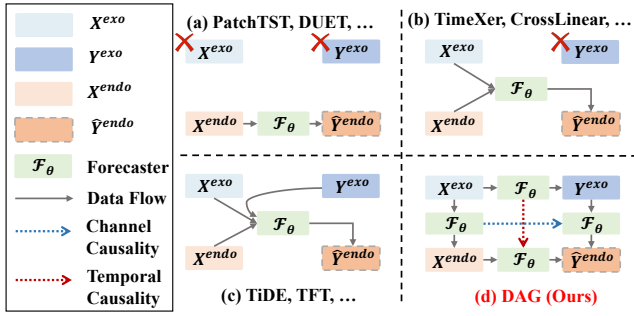


Figure 1: Time series forecasting algorithms can be classified as follows: (a) univariate/multivariate algorithms without exogenous variables, e.g., PatchTST [36] and DUET [45]; (b) algorithms considering only historical exogenous variables, e.g., TimeXer [56] and CrossLinear [67]; (c) algorithms that account for both historical and future exogenous variables, e.g., TiDE [8] and TFT [24]; and (d) algorithms that consider both exogenous variables and causal relationships.

planning. Although these covariates are not part of the prediction target itself, they often contain strong predictive signals.

From a temporal perspective, covariates can be categorized into two types: historical exogenous variables, which are exogenous information observed during the historical period, and future exogenous variables, which are exogenous information available at the forecasting time for future time steps. Despite their high predictive value, current deep learning approaches still underutilize future exogenous variables. As shown in Figure 1, existing exogenous-aware forecasting methods can be broadly divided into the following two categories: 1) Methods using only historical information (Figure 1b): These approaches rely solely on historical endogenous and exogenous variables to forecast future endogenous variables. Representative models include TimeXer [56] and CrossLinear [67]. By entirely ignoring future covariates, these methods may underperform in scenarios where such information is available in advance. 2) Methods that use both historical and future exogenous variables (Figure 1c): For instance, TiDE [8] and TFT [24] use historical information and future exogenous variables to forecast future endogenous variables. However, without causal constraints, such approaches are susceptible to spurious correlations.

Further analysis, as illustrated in Figure 2, reveals that forecasting with known future covariates involves causal dependencies across both temporal and channel dimensions. Temporally, the influence of historical exogenous variables on future exogenous variables mirrors the evolution from historical to future endogenous variables. In terms of channels, the interaction patterns between historical exogenous and endogenous variables are often transferable to those between future exogenous and endogenous variables. This dual causality structure remains an underexplored but critical feature that is insufficiently addressed by existing methods.

Based on the analysis of existing work and our observations in real-world data, we propose a general framework, DAG, which utilizes *Dual Causal network along both the temporal and channel dimensions for time series forecasting with exogenous variables*,

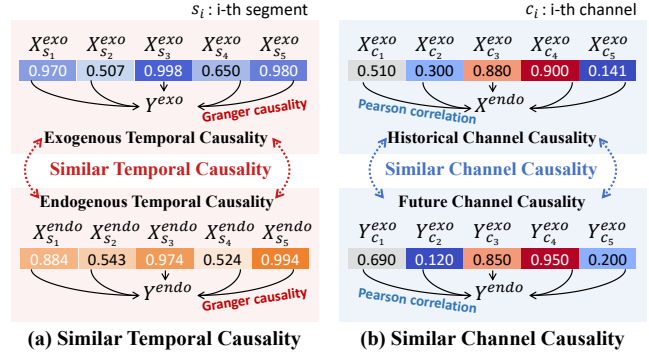


Figure 2: Diagram of Temporal Causality and Channel Causality. Granger causality is used to measure the correlation between historical data and future data. Pearson correlation is used to measure the correlation between exogenous and endogenous variables.

enabling high-quality predictions of future endogenous variables. Specifically, we first introduce the *Temporal Causal Module*. Since the influence of historical exogenous variables on future exogenous variables structurally resembles the evolution of historical endogenous variables into future endogenous variables, we design a causal discovery module to capture how historical exogenous variables affect future exogenous variables. We then construct a causal injection module that incorporates the discovered causal relationships into the process of forecasting future endogenous variables based on historical endogenous variables. Next, we propose the *Channel Causal Module*, which follows a similar design principle, where a causal discovery module models how historical exogenous variables influence historical endogenous variables, and a causal injection module incorporates the discovered relationships to enhance the prediction of future endogenous variables based on future exogenous variables. Finally, we combine the temporal causality loss, channel causality loss, and the forecasting loss of future endogenous variables as the overall *loss function*, enabling end-to-end optimization of the forecasting task.

Our contributions are summarized as:

- We propose a general framework called DAG, which improves forecasting accuracy by discovering and injecting causal relationships across both temporal and channel dimensions, fully leveraging exogenous variables.
- We design a causal discovery module to capture how historical exogenous variables influence future exogenous variables and how they affect historical endogenous variables.
- We design a causal injection module that integrates the discovered temporal and channel causal relationships into the forecasting process of future endogenous variables.
- We open-source our own collected TSF-X datasets and conduct extensive experiments on both public and newly released datasets. The results demonstrate that DAG outperforms state-of-the-art methods.

2 Related works

2.1 Univariate and Multivariate Forecasting

Existing time series forecasting models are typically classified into univariate and multivariate forecasting methods based on the number of input and output variables. **Univariate time series forecasting models** rely solely on the historical values of a single variable to predict future values. Traditional univariate forecasting methods, such as ARIMA [2], ETS [16], and Theta [9] are classical and widely used techniques. However, these methods still depend on manual feature engineering and model design, which limits their flexibility and automation. With the rapid advancement of deep learning technologies [21, 22, 31–33, 55, 64, 69], methods like N-BEATS [38] and DeepAR [46] can automatically learn patterns from historical data, excelling at capturing nonlinear relationships and long-term dependencies. On the other hand, **multivariate time series forecasting models** use multiple input variables to predict the corresponding output variables. The classic methods include VAR [11], Random Forests [3] and LightGBM [17]. In recent years, with the rise of deep learning, various architectural approaches have gained widespread attention. For instance, Transformer architectures, such as Informer [66], FEDformer [68], Autoformer [59], Triformer [5], and PatchTST [36], can more accurately capture the complex relationships between temporal tokens. MLP-based methods, such as SparseTSF [25], CycleNet [26], DUET [45], NLinear [65], and DLinear [65], utilize simpler architectures with fewer parameters but still achieve highly competitive forecasting accuracy. However, all those methods overlook an important practical factor—exogenous (historical or future exogenous). In many real-world scenarios, exogenous data is known or can be approximately known, and utilizing exogenous data can significantly improve the accuracy of predictions.

2.2 Forecasting with Exogenous Variables

Time series forecasting with exogenous variables has been extensively discussed in classical statistical methods. Some statistical methods have been extended to incorporate exogenous variables as part of the input. Methods like ARIMAX [58] and SARIMAX [52] have long utilized exogenous variables to enhance forecasting accuracy. More recently, deep learning approaches have advanced this area: CrossLinear [67] uses cross-correlation embeddings to capture dependencies between historical endogenous and exogenous variables; NBEATSx [37] extends N-BEATS with dedicated branches to utilize both past and future exogenous inputs; TiDE [8] employs an MLP-based architecture to integrate static and future covariates by concatenation with endogenous features at each time step. The Temporal Fusion Transformer (TFT) [24] integrates historical and current exogenous variables using attention mechanisms. Furthermore, TimeXer [56] introduces patch-wise embeddings to flexibly incorporate exogenous covariates without strict temporal alignment. On the other hand, ExoTST [50] utilizes innovative embedding, cross-attention, and cross-temporal fusion within an attention framework to robustly handle time lags and missing data. However, these methods generally rely on relatively simple combinations of historical inputs and future exogenous, without fully modeling the complex interactions among historical endogenous, historical exogenous, and future exogenous variables.

3 Preliminaries

3.1 Definitions

Definition 3.1 (Time Series). A time series $Z \in \mathbb{R}^{N \times T}$ contains T equal-spaced time points with N channels. If $N = 1$, the time series is called univariate; otherwise, it is multivariate when $N > 1$. For clarity, we denote $X_{i,j}$ as the j -th time point of the i -th channel.

Definition 3.2 (Endogenous Time Series). An endogenous time series, denoted as $X^{\text{endo}} \in \mathbb{R}^{N \times T}$, refers to the primary target variable(s) whose future values we aim to forecast. These variables are determined by internal system dynamics and may depend on their own past as well as other external inputs.

Definition 3.3 (Exogenous Time Series). An exogenous time series refers to covariate variables that are not the direct forecasting targets but may influence the endogenous time series. These variables are often known or can be estimated in advance, such as weather, calendar events, or holidays. We denote the exogenous variates as two parts: the *past exogenous variables* $X^{\text{exo}} \in \mathbb{R}^{D \times T}$ and the *future exogenous variables* $Y^{\text{exo}} \in \mathbb{R}^{D \times F}$, where D is the number of exogenous variates, T is the number of past time steps, and F is the forecasting horizon.

3.2 Problem Statement

Exogenous-Aware Time Series Forecasting. Given a historical endogenous time series $X^{\text{endo}} \in \mathbb{R}^{N \times T}$, along with corresponding past exogenous variables $X^{\text{exo}} \in \mathbb{R}^{D \times T}$ and future exogenous variables $Y^{\text{exo}} \in \mathbb{R}^{D \times F}$, the objective is to predict the future values of the endogenous time series over a forecasting horizon of length F . Formally, the goal is to design a function \mathcal{F}_θ parameterized by θ , which models the input time series to get the forecasted future:

$$\hat{Y}^{\text{endo}} = \mathcal{F}_\theta(X^{\text{endo}}, X^{\text{exo}}, Y^{\text{exo}})$$

where $\hat{Y}^{\text{endo}} \in \mathbb{R}^{N \times F}$ denotes the predicted future endogenous variables.

4 Methodology

4.1 Structure Overview

Figure 3 illustrates the overall architecture of DAG, which effectively improves forecasting accuracy by discovering and injecting causal relationships along both the temporal and channel dimensions, thereby fully leveraging the information contained in exogenous variables. Specifically, we first introduce the *Temporal Causal Module*. Since the influence of historical exogenous variables on future exogenous variables structurally resembles the evolution of historical endogenous variables into future endogenous variables, we design a causal discovery module to capture how historical exogenous variables affect future exogenous variables. We then construct a causal injection module that incorporates the discovered causal relationships into the process of forecasting future endogenous variables based on historical endogenous variables. Next, we propose the *Channel Causal Module*, which follows a similar design principle, where a causal discovery module models how historical exogenous variables influence historical endogenous variables, and a causal injection module incorporates the discovered relationships to enhance the prediction of future endogenous variables based on future exogenous variables. Finally, we combine the temporal

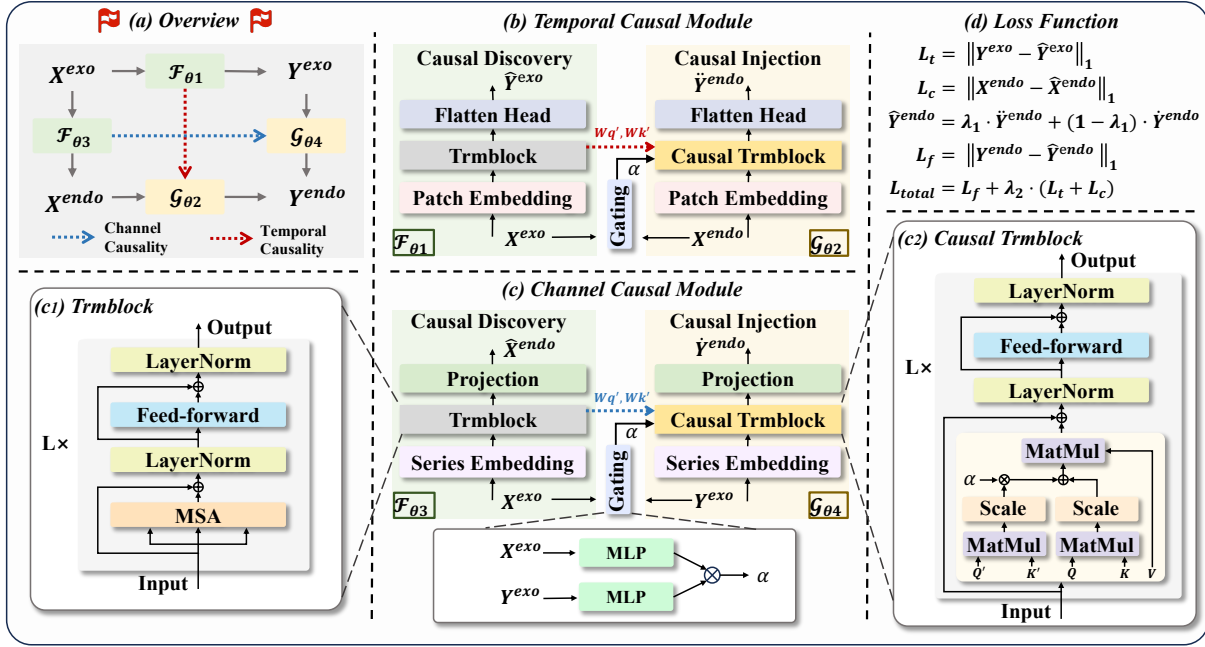


Figure 3: The architecture of DAG. (a) Overview of the DAG framework, which comprises Temporal Causal Modules (F_{θ_1} and G_{θ_2}) and Channel Causal Modules (F_{θ_3} and G_{θ_4}). (b) Detailed structure of the Temporal Causal Module. (c) Detailed structure of the Channel Causal Module. (c1) The standard Transformer block (Trmblock). (c2) The Causal Trmblock, which injects learned causality into the Trmblock. (d) The loss function. Note that the Gating, Trmblock, and Causal Trmblock used in (b) and (c) share the same architecture.

causal loss, channel causal loss, and the forecasting loss of future endogenous variables as the overall *loss function*, enabling end-to-end optimization of the forecasting task.

4.2 Temporal Causality Module

As analyzed in Section 1, the influence mechanism of historical exogenous variables on future exogenous variables shares a structural similarity with the evolution process from historical endogenous variables to future endogenous variables. Therefore, the *Temporal Causality Module* is designed to uncover the causal relationships between historical and future exogenous variables (*Temporal Causal Discovery Module*), and to inject the discovered causality into the modeling process of forecasting future endogenous variables based on historical endogenous variables (*Temporal Causal Injection Module*), thereby improving prediction accuracy.

4.2.1 Temporal Causal Discovery. To extract the causal relationships between historical and future exogenous variables, the *Temporal Causal Discovery Module* adopts a patch-wise representation strategy [6, 36]. Specifically, each historical exogenous variable is segmented into multiple patches, and each patch is projected into a temporal token.

$$S_i = \text{PatchEmbedding}(\text{Patchify}(X_i^{exo}, i \in \{1, \dots, D\})), \quad (1)$$

where $S_i = [s_{i,1}, s_{i,2}, \dots, s_{i,M}] \in \mathbb{R}^{M \times d}$ denotes the all tokens of the i -th channel. M is the number of patches. $s_{i,j} \in \mathbb{R}^d$ denotes the j -th token of i -th channel. PatchEmbedding maps each patch, added by

its position embedding, into a d -dimensional vector via a trainable linear projector. We then employ a standard Transformer block to model the influence weights of different patches on the future exogenous variable.

$$Q = S_i \cdot W_{q'}, K = S_i \cdot W_{k'}, V = S_i \cdot W_{v'} \quad (2)$$

$$\text{score} = \sigma\left(\frac{Q \cdot K^T}{\sqrt{d}}\right) \quad (3)$$

$$S'_i = \text{score} \cdot V, \quad (4)$$

where $S'_i \in \mathbb{R}^{M \times d}$ is the representations processed by MSA and σ is the softmax operation.

To enhance robustness, instead of directly passing the generated attention score to the Temporal Causal Injection Module, we extract and transfer the learnable parameters—specifically the query ($W_{q'}$) and key ($W_{k'}$) matrices—of the Multi-Head Self-Attention (MSA) mechanism that generates the attention score. These parameters serve as the temporal causality representation to be injected.

Finally, the temporal tokens S'_i are then processed by FeedForward layer to obtain $\hat{S}_i \in \mathbb{R}^{M \times d}$ and then fed into a flatten prediction head to forecast future exogenous variables \hat{Y}^{exo} .

$$\hat{Y}^{exo} = \text{Linear}(\text{Flatten}(\hat{S}_i)) \quad (5)$$

The prediction loss of the future exogenous variables is used as the temporal causality loss during training:

$$L_t = \|Y^{exo} - \hat{Y}^{exo}\|_1 \quad (6)$$

4.2.2 Temporal Causal Injection. Consistent with the approach used in the *Temporal Causal Discovery Module*, we first obtain patch-wise representations of the historical endogenous variables.

$$P_i = \text{PatchEmbedding}(\text{Patchify}(X_i^{\text{endo}}, i \in \{1, \dots, N\})), \quad (7)$$

where $P_i = [p_{i,1}, p_{i,2}, \dots, p_{i,M}] \in \mathbb{R}^{M \times d}$ denotes the all tokens of the i -th channel. $p_{i,j} \in \mathbb{R}^d$ denotes the j -th token of i -th channel.

Then, we employ the Causal Transformer Block to model the influence of different endogenous variable patches on the future endogenous variable, while incorporating the causal information passed from the *Temporal Causal Discovery Module*. Specifically, in the attention mechanism, the input tokens are projected via original query and key matrices (W_q, W_k and W_v) within the Causal Trmblock to obtain Q, K and V , and simultaneously through ($W_{q'}, W_{k'}$ and $W_{v'}$) extracted from the Temporal Causal Discovery Module to generate Q' and K' .

$$Q' = P_i \cdot W_{q'}, K' = P_i \cdot W_{k'} \quad (8)$$

$$Q = P_i \cdot W_q, K = P_i \cdot W_k, V = P_i \cdot W_v \quad (9)$$

We then compute two sets of attention scores, followed by scaling and softmax operations (σ). A learnable weighting factor α is then introduced to fuse the two attention scores, resulting in the final fused attention score. This mechanism explicitly injects temporal causal structure into the attention computation, enabling the model to capture causally informed dependencies among tokens along the temporal dimension.

$$\text{FusedScore} = \alpha \cdot \sigma\left(\frac{Q \cdot K^T}{\sqrt{d}}\right) + (1 - \alpha) \cdot \sigma\left(\frac{Q' \cdot K'^T}{\sqrt{d}}\right) \quad (10)$$

$$P'_i = \sigma(\text{FusedScore}) \cdot V \quad (11)$$

Gating Mechanism: To adaptively weight the two sets of attention scores along the temporal dimension, we design a Gating mechanism—see Equation 12. This module takes the historical exogenous variables X^{exo} and the historical endogenous variables X^{endo} as input, and encodes them through two separate multilayer perceptrons (MLPs) to obtain nonlinear representations. The outputs of the two MLPs are then fused via a dot product operation to produce a scalar weight α . This weight α is used to adaptively combine the attention scores, guiding the model to integrate information dynamically based on the actual influence strength between historical exogenous and endogenous variable, thereby improving modeling accuracy and robustness.

$$\alpha = \text{MLP}(X_i^{\text{exo}})^T \cdot \text{MLP}(X_i^{\text{endo}}) \quad (12)$$

Finally, the temporal tokens P'_i output by the Attention mechanism are then processed by Feedforward layer to obtain $\hat{P}_i \in \mathbb{R}^{F \times d}$ and fed into the flatten prediction head to generate forecasts of future endogenous variables.

$$\hat{Y}_i^{\text{endo}} = \text{Linear}(\text{Flatten}(\hat{P}_i)) \quad (13)$$

4.3 Channel Causality Module

Similar to the temporal dimension, the *Channel Causality Module* aims to model and inject causal relationships along the variable (channel) dimension. This module focuses on how historical exogenous variables influence historical endogenous variables and how

such causal patterns can be transferred to enhance the prediction of future endogenous variables using future exogenous variables.

4.3.1 Channel Causal Discovery. To capture the causal effects from historical exogenous variables to historical endogenous variables, the *Channel Causal Discovery Module* employs a series-wise representation. Specifically, we encode each historical exogenous variables X_i^{exo} over time into a series-wise token through a series embedding layer.

$$U = \text{SeriesEmbedding}(X_i^{\text{exo}}, i \in \{1, \dots, D\}), \quad (14)$$

The embedded historical exogenous variables $U = [u_1, u_2, \dots, u_D] \in \mathbb{R}^{D \times d}$ are then fed into a standard Transformer block (Trmblock):

$$Q = U \cdot W_{q'}, K = U \cdot W_{k'}, V = U \cdot W_{v'} \quad (15)$$

$$U' = \sigma\left(\frac{Q \cdot K^T}{\sqrt{d}}\right) \cdot V, \quad (16)$$

then the series token U' is processed through FeedForward layer and obtain $\hat{U} \in \mathbb{R}^{D \times d}$ and passed through a projection layer to generate a prediction \hat{X}^{endo} for the historical endogenous variables:

$$\hat{X}^{\text{endo}} = \text{Linear}(\text{MLP}(\hat{U})) \quad (17)$$

Similar to Section 4.2.1, the Channel Causal Discovery Module serves two purposes: (1) it is used to define the channel causality loss, and (2) its underlying attention mechanism's learnable parameters (query and key matrices $W_{q'}$ and $W_{k'}$) are extracted to be injected into the following channel causal injection module.

The prediction loss of the historical endogenous variables is used as the temporal causality loss during training:

$$L_c = \left\| X^{\text{endo}} - \hat{X}^{\text{endo}} \right\|_1 \quad (18)$$

4.3.2 Channel Causal Injection. This module uses future exogenous variables to predict future endogenous variables, while incorporating the channel-level causal representations extracted in the previous step. First, the future exogenous variables are encoded using the same series embedding strategy:

$$O = \text{SeriesEmbedding}(Y_i^{\text{exo}}, i \in \{1, \dots, D\}), \quad (19)$$

The Causal Trmblock is then used to model channel dependencies while injecting learned causal information.

$$Q' = O \cdot W_{q'}, K' = O \cdot W_{k'} \quad (20)$$

$$Q = O \cdot W_q, K = O \cdot W_k, V = O \cdot W_v \quad (21)$$

$$\alpha = \text{MLP}(X^{\text{exo}})^T \cdot \text{MLP}(Y^{\text{exo}}) \quad (22)$$

$$\text{FusedScore} = \alpha \cdot \sigma\left(\frac{Q \cdot K^T}{\sqrt{d}}\right) + (1 - \alpha) \cdot \sigma\left(\frac{Q' \cdot K'^T}{\sqrt{d}}\right) \quad (23)$$

$$O' = \sigma(\text{FusedScore}) \cdot V \quad (24)$$

Gating Mechanism: Similar to the gating mechanism in Section 4.2.2. This gating mechanism takes the historical exogenous variable X^{exo} and future exogenous variable Y^{exo} as input, and encodes them using two separate MLPs. The outputs of the two MLPs are then fused via a dot product operation to compute a scalar weight α . This weight α is subsequently used to adaptively combine the attention scores, dynamically adjusting the model's focus on the historical and future exogenous information based on their relative influence strength.

The final fused attention is then used to refine the representation of the series token. The refined tokens are processed through Feed-Forward layer to obtain \hat{O} and then passed into the prediction head to generate a prediction \hat{Y}^{endo} for the future endogenous variables:

$$\hat{Y}^{endo} = \text{Linear}(\text{MLP}(\hat{O})) \quad (25)$$

4.4 Loss Function

The training objective of DAG consists of three components: 1) the *temporal causality loss* L_t introduced in Section 4.2.1, which measures how well the model captures temporal causal structures when forecasting future exogenous variables. 2) the *channel causality loss* L_c from Section 4.3.1, which reflects the modeling error in capturing the causal relationships between historical exogenous and endogenous variables. 3) the final *forecasting loss* L_f for future endogenous variables, computed based on the fused prediction, which evaluates the final prediction accuracy of the target variables.

To obtain the final prediction for future endogenous variables, we fuse two candidate predictions using a fusion weight λ_1 :

$$\hat{Y}^{endo} = \lambda_1 \cdot \check{Y}^{endo} + (1 - \lambda_1) \cdot \dot{Y}^{endo}, \quad (26)$$

where \check{Y}^{endo} and \dot{Y}^{endo} are prediction outputs from Temporal Causal Injection Module and Channel Causal Injection Module.

The forecasting loss is defined as:

$$L_f = \left\| Y^{endo} - \hat{Y}^{endo} \right\|_1 \quad (27)$$

Finally, the total loss function combines the forecasting loss with the causality-related losses:

$$L_{total} = L_f + \lambda_2 \cdot (L_t + L_c), \quad (28)$$

where λ_2 is a causality weight that balances the contribution of causality modeling during training.

5 Experiments

5.1 Experimental Settings

5.1.1 Datasets. To ensure comprehensive and fair comparisons across different models, 1) we perform experiments on eight common multivariate forecasting datasets (ETT with 4 subsets, Weather, Exchange, Electricity, and Traffic). Notably, although the future exogenous variables in these datasets are not known, we conduct vanilla forecasting with exogenous variables by treating the last dimension of the multivariate data as the endogenous series and the remaining dimensions as exogenous variables. 2) Additionally, we conduct experiments on 12 real-world datasets that satisfy the TSF-X conditions, including 5 EPF [19, 56] datasets and 7 datasets we sourced ourselves. The future exogenous variables in these datasets are either approximately known or highly accurate. More details about the datasets are provided in Appendix A.1, Table 5.

5.1.2 Baselines. We comprehensively compare our model against 10 baselines, including 1) methods that inherently support future exogenous variables, such as TimeXer [56], TFT [24], and TiDE [8], 2) as well as methods that do not originally support future exogenous variables, like DUET [45], CrossLinear [67], Amplifier [10], TimeKAN [14], xPatch [48], PatchTST [36], and DLinear [65]. For methods that do not support future covariates, we adapt them to incorporate future exogenous variables using an MLP fusion

approach—see Algorithm 1 in Appendix A.3. Note that, for fairness, all methods in our experiments use historical endogenous variables, historical exogenous variables, and future exogenous variables.

5.2 Main Results

Comprehensive forecasting results are presented in Table 1 and Table 2 to demonstrate the performance of DAG on the TSF-X task. We have the following observations:

1) Compared with forecasters of various structures, DAG achieves outstanding predictive performance. In terms of absolute metrics, Table 1 shows that DAG surpasses the second-best baseline, TimeXer, with a 10.8% reduction in MSE and a 6.4% reduction in MAE. Likewise, in Table 2, DAG achieves the highest number of first-place rankings—26 for MSE and 29 for MAE—demonstrating clear superiority over other methods such as TimeXer and TFT.

2) Methods that natively support future exogenous variables (e.g., TiDE, TFT, TimeXer) generally perform better than those that do not (e.g., PatchTST, DLinear), even when enhanced via MLP fusion. DAG, by explicitly modeling causal relationships while leveraging exogenous inputs, not only competes with these top baselines but surpasses them in nearly all metrics. This demonstrates the strength of incorporating causality-aware mechanisms in TSF-X tasks.

5.3 Model Analyses

5.3.1 Ablation Studies. We compare the full version of DAG with the following variants across four datasets. The Electricity has a lookback length of 96 and forecasts 720 steps, while the other three datasets have a lookback length of 720 steps and forecast 360 steps—see Table 3.

- (a) \mathcal{G}_{θ_2} : Uses only X^{endo} to predict Y^{endo} .
- (b) \mathcal{G}_{θ_4} : Uses only Y^{exo} to predict Y^{endo} .
- (c) $\mathcal{G}_{\theta_2} + \mathcal{G}_{\theta_4}$: Uses both X^{endo} and Y^{exo} to predict Y^{endo} .
- (d) $\mathcal{F}_{\theta_1} + \mathcal{G}_{\theta_2}$ + Temporal Causality: Predicts Y^{endo} using X^{endo} while incorporating temporal causality and the corresponding temporal causality loss derived from predicting Y^{exo} using X^{exo} .
- (e) $\mathcal{F}_{\theta_3} + \mathcal{G}_{\theta_4}$ + Channel Causality: Predicts Y^{endo} using Y^{exo} while incorporating channel causality and the corresponding channel causality loss derived from predicting X^{endo} using X^{exo} .

We make the following observations: 1) using only historical endogenous variables \mathcal{G}_{θ_2} or only future exogenous variables \mathcal{G}_{θ_4} results in suboptimal forecasting performance, indicating that relying on a single input source is insufficient for high-quality predictions. 2) Combining both $\mathcal{G}_{\theta_2} + \mathcal{G}_{\theta_4}$ leads to a significant performance improvement, highlighting their complementary roles in modeling. 3) Furthermore, introducing temporal causality module ($\mathcal{F}_{\theta_1} + \mathcal{G}_{\theta_2}$ + Temporal Causality) improves performance compared to using only historical endogenous variables \mathcal{G}_{θ_2} ; similarly, incorporating channel causality module ($\mathcal{F}_{\theta_3} + \mathcal{G}_{\theta_4}$ + Channel Causality) outperforms the variant that uses only future exogenous variables \mathcal{G}_{θ_4} . These results validate the effectiveness of both causality modeling mechanisms in DAG. 4) Ultimately, the full DAG model, which integrates both temporal and channel causality, achieves the best results, demonstrating the importance of modeling dual causality structures for TSF-X tasks.

5.3.2 Parameter Sensitivity. We also conduct parameter sensitivity studies of DAG. We make the following observations: 1) Figure 4a

Table 1: Average results on common multivariate datasets for the TSF-X task, where the inputs are (X^{endo} , X^{exo} , and Y^{exo}). Red: the best, Blue: the 2nd best. Full results are provided in Table 6 of Appendix B.1.

Models Metrics	DAG (ours)		TimeXer		TFT		TiDE		DUET		CrossLinear		Amplifier		TimeKAN		xPatch		PatchTST		DLinear	
	mse	mae	mse	mae	mse	mae	mse	mae	mse	mae	mse	mae	mse	mae	mse	mae	mse	mae	mse	mae	mse	mae
ETTh1	0.071	0.206	0.081	0.219	0.094	0.239	<u>0.079</u>	<u>0.217</u>	0.225	0.396	0.216	0.388	0.180	0.344	0.177	0.335	0.165	0.328	0.236	0.407	0.235	0.404
ETTh2	0.183	0.335	0.199	0.350	0.261	0.409	0.195	<u>0.344</u>	0.198	0.352	0.197	0.354	0.219	0.372	0.207	0.362	<u>0.185</u>	0.348	0.200	0.358	0.192	0.348
ETTm1	0.052	0.172	<u>0.054</u>	<u>0.175</u>	0.060	0.185	0.055	0.178	0.199	0.375	0.194	0.372	0.192	0.367	0.169	0.332	0.146	0.312	0.183	0.358	0.187	0.349
ETTm2	0.117	0.253	0.128	0.267	0.193	0.338	<u>0.119</u>	<u>0.256</u>	0.148	0.307	0.163	0.326	0.167	0.330	0.159	0.318	0.148	0.302	0.157	0.321	0.139	0.294
Weather	0.002	0.026	0.001	<u>0.027</u>	0.002	0.031	0.002	0.030	<u>0.002</u>	0.029	0.008	0.074	0.011	0.083	0.007	0.067	0.002	0.029	0.009	0.076	0.010	0.080
Electricity	0.194	0.329	<u>0.208</u>	<u>0.337</u>	0.375	0.471	0.313	0.417	0.281	0.411	0.264	0.399	0.277	0.413	0.301	0.429	0.265	0.400	0.269	0.404	0.288	0.420
Traffic	0.129	0.203	0.142	0.238	<u>0.132</u>	<u>0.220</u>	0.154	0.255	0.263	0.322	0.232	0.291	0.194	0.276	0.211	0.285	0.221	0.287	0.233	0.295	0.212	0.281
Exchange	0.212	0.353	<u>0.250</u>	<u>0.380</u>	0.334	0.438	0.293	0.398	0.270	0.455	0.312	0.494	0.298	0.463	0.425	0.565	0.298	0.463	0.464	0.618	0.363	0.510

Table 2: Results on 12 real-world datasets that satisfy the TSF-X task, where the inputs are (X^{endo} , X^{exo} , and Y^{exo}). Red: the best, Blue: the 2nd best. Avg means the average results from two forecasting horizons. Experimental setup is detailed in Section A.2.

Models Metrics	DAG (ours)		TimeXer		TFT		TiDE		DUET		CrossLinear		Amplifier		TimeKAN		xPatch		PatchTST		DLinear		
	mse	mae	mse	mae	mse	mae	mse	mae	mse	mae	mse	mae	mse	mae	mse	mae	mse	mae	mse	mae	mse	mae	
NP	24	0.202	0.237	0.236	0.266	0.219	<u>0.249</u>	0.284	0.301	0.246	0.287	<u>0.210</u>	0.266	0.252	0.303	0.273	0.310	0.234	0.278	0.249	0.294	0.282	0.337
	360	0.521	0.451	0.600	0.475	0.539	0.501	0.601	0.498	0.576	0.528	0.531	0.508	0.587	0.534	0.538	0.529	<u>0.523</u>	<u>0.461</u>	0.530	0.498	0.601	0.552
	Avg	0.362	0.344	0.418	0.371	0.379	0.375	0.443	0.400	0.411	0.408	<u>0.371</u>	0.387	0.420	0.418	0.405	0.419	0.378	<u>0.370</u>	0.390	0.396	0.442	0.444
PJM	24	0.057	0.143	0.075	<u>0.166</u>	0.095	0.195	0.106	0.214	<u>0.072</u>	0.166	0.088	0.191	0.096	0.208	0.115	0.244	0.077	0.168	0.116	0.239	0.096	0.208
	360	0.130	0.218	0.140	0.231	0.133	<u>0.219</u>	0.177	0.279	<u>0.131</u>	0.228	0.135	0.254	0.177	0.285	0.162	0.281	0.131	0.220	0.149	0.279	0.164	0.278
	Avg	0.093	0.180	0.108	0.198	0.114	0.207	0.142	0.246	<u>0.102</u>	0.197	0.112	0.223	0.137	0.246	0.139	0.262	0.104	<u>0.194</u>	0.133	0.259	0.130	0.243
BE	24	0.361	0.229	0.392	<u>0.253</u>	0.426	0.272	0.426	0.285	0.432	0.272	<u>0.391</u>	0.259	0.471	0.339	0.451	0.319	0.411	0.256	0.452	0.326	0.451	0.310
	360	0.485	0.330	0.512	<u>0.327</u>	0.482	0.310	0.571	0.364	0.597	0.436	0.568	0.416	0.646	0.487	0.645	0.495	0.579	0.410	0.702	0.538	0.600	0.442
	Avg	0.423	0.279	<u>0.452</u>	<u>0.290</u>	0.454	0.291	0.498	0.325	0.515	0.354	0.479	0.337	0.559	0.413	0.548	0.407	0.495	0.333	0.577	0.432	0.526	0.376
FR	24	0.355	0.171	<u>0.366</u>	<u>0.208</u>	0.543	0.253	0.418	0.255	0.384	0.251	0.390	0.226	0.459	0.348	0.454	0.296	0.424	0.235	0.518	0.368	0.422	0.265
	360	0.473	0.268	0.489	0.273	0.465	0.261	0.551	0.308	0.607	0.403	0.575	0.370	0.648	0.468	0.641	0.452	0.556	0.350	0.658	0.452	0.572	0.362
	Avg	0.414	0.219	<u>0.427</u>	<u>0.241</u>	0.504	0.257	0.484	0.281	0.496	0.327	0.483	0.298	0.554	0.408	0.547	0.374	0.490	0.293	0.588	0.410	0.497	0.314
DE	24	0.277	0.322	<u>0.339</u>	<u>0.362</u>	0.380	0.383	0.367	0.383	0.376	0.378	0.387	0.396	0.394	0.407	0.399	0.412	0.399	0.394	0.413	0.412	0.423	0.426
	360	0.462	0.418	0.610	0.474	0.599	0.509	0.630	0.511	0.589	0.482	0.583	0.507	0.551	0.474	<u>0.547</u>	0.479	0.550	<u>0.472</u>	0.589	0.498	0.573	0.487
	Avg	0.370	0.370	0.475	<u>0.418</u>	0.489	0.446	0.499	0.447	0.482	0.430	0.485	0.452	0.473	0.441	<u>0.473</u>	0.445	0.474	0.433	0.501	0.455	0.498	0.457
Energy	24	0.079	0.215	0.122	0.273	0.093	0.235	0.103	0.248	0.117	0.283	0.241	0.418	0.138	0.306	0.135	0.298	0.092	0.240	0.239	0.390	<u>0.085</u>	<u>0.230</u>
	360	0.169	0.320	0.204	0.357	0.167	<u>0.331</u>	0.202	0.355	0.288	0.452	0.237	0.385	0.328	0.472	0.302	0.464	0.204	0.367	0.214	0.363	0.263	0.416
	Avg	0.124	0.267	0.163	0.315	<u>0.130</u>	<u>0.283</u>	0.153	0.302	0.203	0.367	0.239	0.402	0.233	0.389	0.218	0.381	0.148	0.303	0.226	0.377	0.174	0.323
Sdwpfm1	24	0.351	0.400	0.558	0.533	0.366	<u>0.421</u>	0.474	0.488	0.551	0.564	<u>0.355</u>	0.473	0.364	0.445	0.418	0.503	0.669	0.580	0.374	0.454	0.417	0.501
	360	0.495	0.522	0.845	0.684	0.597	0.528	0.492	<u>0.526</u>	0.646	0.577	0.497	0.532	0.510	0.535	0.476	0.566	0.592	0.556	0.497	0.550	<u>0.480</u>	0.562
	Avg	0.423	0.461	0.701	0.609	0.482	<u>0.474</u>	0.483	0.507	0.599	0.570	<u>0.426</u>	0.502	0.437	0.490	0.447	0.534	0.630	0.568	0.435	0.502	0.449	0.531
Sdwpfm2	24	0.372	0.414	0.627	0.570	0.411	0.458	0.461	0.492	0.445	<u>0.452</u>	0.477	0.536	<u>0.394</u>	0.462	0.474	0.538	0.508	0.478	0.418	0.492	0.459	0.530
	360	0.583	0.556	0.978	0.736	0.541	<u>0.519</u>	0.511	0.540	0.584	0.528	0.589	0.611	0.587	0.563	<u>0.520</u>	0.589	0.523	0.513	0.602	0.603	0.589	0.630
	Avg	0.477	0.485	0.803	0.653	0.476	<u>0.488</u>	0.486	0.516	0.514	0.490	0.533	0.573	0.491	0.512	0.497	0.564	0.516	0.495	0.510	0.547	0.524	0.580
Sdwpfh1	24	0.408	0.438	0.651	0.587	0.401	<u>0.460</u>	0.434	0.489	0.527	0.513	0.548	0.585	0.576	0.627	0.511	0.582	0.524	0.505	0.422	0.505	0.557	0.613
	360	0.489	0.534	0.841	0.700	0.557	0.523	<u>0.472</u>	0.527	0.551	<u>0.519</u>	0.566	0.601	0.497	0.569	0.643	0.694	0.472	0.504	0.513	0.548	0.600	0.635
	Avg	0.448	0.486	0.746	0.643	0.479	<u>0.491</u>	<u>0.453</u>	0.508	0.539	0.516	0.557	0.593	0.537	0.598	0.577	0.638	0.498	0.505	0.468	0.527	0.579	0.624
Sdwpfh2	24	0.438	0.465	0.820	0.677	0.474	<u>0.493</u>	0.579	0.553	0.629	0.563	0.468	0.540	0.473	0.533	0.580	0.614	0.640	0.554	<u>0.457</u>	0.527	0.633	0.653
	360	0.608	0.595	0.962	0.761	0.657	<u>0.549</u>	0.619	0.614	0.665	0.569	0.608	0.609	0.569	0.628	0.713	0.729	<u>0.579</u>	0.547	0.641	0.632	0.704	0.674
	Avg	0.523	0.530	0.891	0.719	0.566	0.521	0.599	0.583	0.647	0.566	0.538	0.574	0.521	0.581	0.647	0.672	0.610	0.551	0.549	0.580	0.669	0.664
Colburn	10	0.061	0.094	0.113	0.172	0.092	0.135	0.089	0.131	0.089	0.134	0.071	0.102	0.071	0.121	<u>0.061</u>	<u>0.101</u>	0.090	0.104	0.062	0.122	0.069	0.151
	30	0.135	0.215	<u>0.176</u>	0.299	0.383	0.460	0.240	0.322	0.307	0.397	0.182	0.288	0.275	0.370	0.195	<u>0.249</u>	0.217	0.315	0.417	0.496	0.245	0.285
	Avg	0.098	0.154	0.145	0.235	0.238	0.297	0.164	0.227	0.198	0.266	<u>0.126</u>	0.195	0.173	0.246	0.128	<u>0.175</u>	0.153	0.210	0.2			

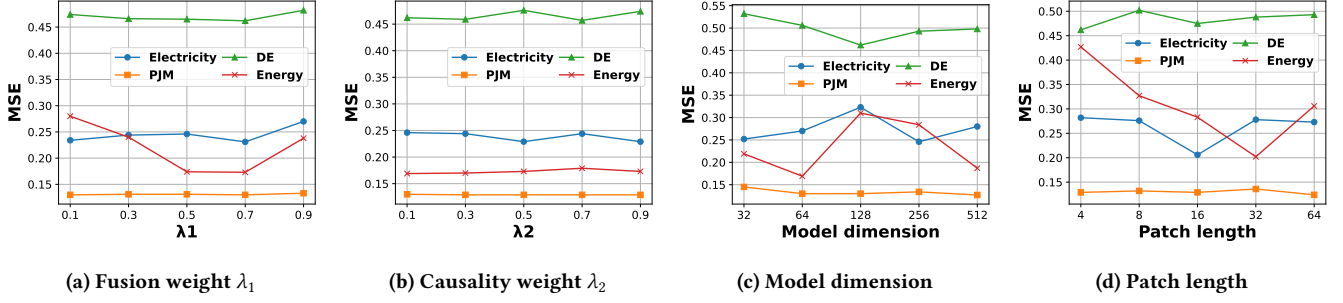


Figure 4: Parameter sensitivity studies of main hyper-parameters in DAG.

Table 3: Ablation studies for DAG.

Datasets	Electricity		PJM		DE		Energy		Average	
	mse	mae								
(a) \mathcal{G}_{θ_1}	0.512	0.514	0.191	0.264	0.846	0.586	0.263	0.408	0.453	0.443
(b) \mathcal{G}_{θ_2}	0.488	0.510	0.169	0.254	0.483	0.443	0.637	0.661	0.444	0.467
(c) $\mathcal{G}_{\theta_1} + \mathcal{G}_{\theta_2}$	0.313	0.412	0.131	0.219	0.480	0.429	0.169	0.320	0.273	0.345
(d) $\mathcal{F}_{\theta_1} + \mathcal{G}_{\theta_2} +$ Temporal Causality	0.504	0.509	0.189	0.261	0.855	0.585	0.240	0.389	0.447	0.436
(e) $\mathcal{F}_{\theta_1} + \mathcal{G}_{\theta_1} +$ Channel Causality	0.392	0.459	0.170	0.255	0.473	0.438	0.350	0.467	0.346	0.405
DAG (ours)	0.246	0.370	0.130	0.218	0.462	0.418	0.169	0.320	0.252	0.331

Table 4: Experimental results under the setting where only historical exogenous variables are used, without future exogenous variables. The inputs are (X^{endo} and X^{exo}). Avg means the average results from two forecasting horizons. Red: the best, Blue: the 2nd best.

Models Datsets	DAG		TimeXer		CrossLinear		DUET		PatchTST		
	mse	mae	mse	mae	mse	mae	mse	mae	mse	mae	
Colburn	10	0.070	0.098	0.084	0.146	0.068	0.101	0.073	0.106	0.083	0.125
	30	0.180	0.223	0.181	0.293	0.190	0.289	0.221	0.290	0.217	0.316
	Avg	0.125	0.160	0.132	0.219	0.129	0.195	0.147	0.198	0.150	0.221
Energy	24	0.117	0.264	0.138	0.293	0.102	0.246	0.108	0.254	0.108	0.254
	360	0.193	0.347	0.206	0.360	0.299	0.425	0.211	0.362	0.298	0.428
	Avg	0.155	0.305	0.172	0.326	0.201	0.336	0.160	0.308	0.203	0.341
DE	24	0.420	0.404	0.501	0.445	0.438	0.423	0.424	0.403	0.503	0.450
	360	0.786	0.564	0.818	0.568	0.832	0.592	0.895	0.623	0.889	0.604
	Avg	0.603	0.484	0.659	0.507	0.635	0.508	0.660	0.513	0.696	0.527
PJM	24	0.072	0.162	0.096	0.191	0.096	0.198	0.082	0.178	0.106	0.212
	360	0.182	0.259	0.186	0.267	0.197	0.283	0.198	0.273	0.189	0.273
	Avg	0.127	0.211	0.141	0.229	0.147	0.241	0.140	0.226	0.148	0.243
NP	24	0.226	0.255	0.270	0.292	0.246	0.282	0.262	0.271	0.283	0.296
	360	0.609	0.505	0.609	0.474	0.655	0.505	0.626	0.494	0.630	0.505
	Avg	0.417	0.380	0.440	0.383	0.451	0.394	0.444	0.383	0.457	0.401

falling between 0.3 and 0.7, indicating that moderate weighting is beneficial for improving performance. 2) Figure 4c shows that model dimension has a certain impact on performance, but DAG maintains good stability across different configurations. Smaller dimensions help reduce computational cost, while dimensions in the range of 64 to 256 generally achieve a good balance between prediction accuracy and model complexity. 3) Figure 4d explores the effect of patch length on model performance. Due to differences in temporal dependencies across datasets, the optimal patch length

varies; however, a patch size between 8 and 32 tends to yield favorable results. It is worth noting that very small patch lengths may lead to increased computational complexity, while excessively large patch lengths may weaken the model’s ability to capture local dependencies.

5.3.3 *Not Using Future Exogenous Variables.* Considering that not all datasets have access to future exogenous variables, we conduct experiments using only historical exogenous variables, excluding future exogenous variables, to validate the practicality of DAG—see Table 4. Specifically, for DAG, during inference, we use the \hat{Y}^{exo} predicted by \mathcal{F}_{θ_1} to replace the actual value Y^{exo} used in \mathcal{G}_{θ_2} for predicting Y^{endo} , thus avoiding the issue of unavailable future exogenous variables. For other baseline models, we also uniformly use only historical exogenous variables. The experimental results show that DAG continues to perform excellently. Methods that consider historical exogenous variable modeling, such as TimeXer and CrossLinear, also perform well. DUET, which flexibly models channel relationships, also achieves good results, while the channel-independent algorithm PatchTST performs poorly.

6 Conclusion

Time series forecasting is crucial in various fields such as economics, traffic, and AIOps. In this study, we propose a general framework **DAG**, which *utilizes Dual Causal network along both the temporal and channel dimensions for time series forecasting with exoGenous variables*, especially leveraging future exogenous variable information. The framework introduces a *Temporal Causal Module* which includes a temporal causal discovery module to model how historical exogenous variables affect future exogenous variables, followed by a causal injection module to incorporate these relationships for forecasting future endogenous variables. Additionally, a Channel Causal Module is introduced. It features a channel causal discovery module to model the impact of historical exogenous variables on historical endogenous variables and injects these relationships for improved forecasting of future endogenous variables based on future exogenous variables. Finally, this framework combines temporal causality loss, channel causality loss, and forecasting loss to enable end-to-end optimization. Extensive experiments show that DAG achieves state-of-the-art performance. Additionally, all datasets and code are available at <https://github.com/decisionintelligence/DAG>.

References

- [1] Francisco Martinez Alvarez, Alicia Troncoso, Jose C Riquelme, and Jesus S Aguilar Ruiz. 2011. Energy Time Series Forecasting Based on Pattern Sequence Similarity. *IEEE Trans. Knowl. Data Eng.* 23, 8 (2011), 1230–1243.
- [2] George EP Box and David A Pierce. 1970. Distribution of residual autocorrelations in autoregressive-integrated moving average time series models. *Journal of the American statistical Association* 65, 332 (1970), 1509–1526.
- [3] Leo Breiman. 2001. Random forests. *Machine learning* 45 (2001), 5–32.
- [4] David Campos, Bin Yang, Tung Kieu, Miao Zhang, Chenjuan Guo, and Christian S Jensen. 2024. QCore: Data-Efficient, On-Device Continual Calibration for Quantized Models—Extended Version. *arXiv preprint arXiv:2404.13990* (2024).
- [5] Razvan-Gabriel Cirstea, Chenjuan Guo, Bin Yang, Tung Kieu, Xuanyi Dong, and Shirui Pan. 2022. Triformer: Triangular, Variable-Specific Attentions for Long Sequence Multivariate Time Series Forecasting. In *IJCAI*. 1994–2001.
- [6] Razvan-Gabriel Cirstea, Chenjuan Guo, Bin Yang, Tung Kieu, Xuanyi Dong, and Shirui Pan. 2022. Triformer: Triangular, Variable-Specific Attentions for Long Sequence Multivariate Time Series Forecasting. In *IJCAI*. 1994–2001.
- [7] Tao Dai, Beiliang Wu, Peiyuan Liu, Naiqi Li, Jigang Bao, Yong Jiang, and Shu-Tao Xia. 2024. Periodicity Decoupling Framework for Long-term Series Forecasting. *International Conference on Learning Representations* (2024).
- [8] Abhimanyu Das, Weihao Kong, Andrew Leach, Shaan Mathur, Rajat Sen, and Rose Yu. 2023. Long-term forecasting with tide: Time-series dense encoder. *arXiv preprint arXiv:2304.08424* (2023).
- [9] Cristian Challú Kin G. Olivares Federico Garza, Max Mergenthaler Canseco. 2022. StatsForecast: Lightning fast forecasting with statistical and econometric models. PyCon Salt Lake City, Utah, US 2022.
- [10] Jingru Fei, Kun Yi, Wei Fan, Qi Zhang, and Zhendong Niu. 2025. Amplifier: Bringing Attention to Neglected Low-Energy Components in Time Series Forecasting. In *AAAI*, Vol. 39. 11645–11653.
- [11] Rakshitha Godahewa, Christoph Bergmeir, Geoffrey I Webb, Rob J Hyndman, and Pablo Montero-Manso. 2021. Monash time series forecasting archive. *arXiv preprint arXiv:2105.06643* (2021).
- [12] Chenjuan Guo, Bin Yang, Ove Andersen, Christian S Jensen, and Kristian Torp. 2015. Ecomark 2.0: empowering eco-routing with vehicular environmental models and actual vehicle fuel consumption data. *Geoinformatica* 19 (2015), 567–599.
- [13] Hans Hersbach, Bill Bell, Paul Berrisford, Shoji Hirahara, András Horányi, Joaquín Muñoz-Sabater, Julien Nicolas, Carole Peubey, Raluca Radu, Dinand Schepers, et al. 2020. The ERA5 global reanalysis. *Quarterly journal of the royal meteorological society* 146, 730 (2020), 1999–2049.
- [14] Songtao Huang, Zhen Zhao, Can Li, and Lei Bai. 2025. Timekan: Kan-based frequency decomposition learning architecture for long-term time series forecasting. In *ICLR*.
- [15] Xuanwen Huang, Yang Yang, Yang Wang, Chunping Wang, Zhisheng Zhang, Jiarong Xu, Lei Chen, and Michalis Vazirgiannis. 2022. DGraph: A Large-Scale Financial Dataset for Graph Anomaly Detection. In *NeurIPS*. 22765–22777.
- [16] Rob Hyndman, Anne B Koehler, J Keith Ord, and Ralph D Snyder. 2008. *Forecasting with exponential smoothing: the state space approach*.
- [17] Guolin Ke, Qi Meng, Thomas Finley, Taifeng Wang, Wei Chen, Weidong Ma, Qiwei Ye, and Tie-Yan Liu. 2017. Lightgbm: A highly efficient gradient boosting decision tree. *Advances in Neural Information Processing Systems* 30 (2017).
- [18] Tung Kieu, Bin Yang, Chenjuan Guo, Christian S. Jensen, Yan Zhao, Feiteng Huang, and Kai Zheng. 2022. Robust and Explainable Autoencoders for Unsupervised Time Series Outlier Detection. In *ICDE*. 3038–3050.
- [19] Jesus Lago, Grzegorz Marcjasz, Bart De Schutter, and Rafał Weron. 2021. Forecasting day-ahead electricity prices: A review of state-of-the-art algorithms, best practices and an open-access benchmark. *Applied Energy* 293 (2021), 116983.
- [20] Chonho Lee, Zhaojing Luo, Kee Yuan Ngiam, Meihui Zhang, Kaiping Zheng, Gang Chen, Beng Chin Ooi, and Wei Luen James Yip. 2017. Big healthcare data analytics: Challenges and applications. *Handbook of large-scale distributed computing in smart healthcare* (2017), 11–41.
- [21] Leyang Li, Shilin Lu, Yan Ren, and Adams Wai-Kin Kong. 2025. Set you straight: Auto-steering denoising trajectories to sidestep unwanted concepts. *arXiv preprint arXiv:2504.12782* (2025).
- [22] Xiang Li, Yangfan He, Shuaishuai Zu, Zhengyang Li, Tianyu Shi, Yiting Xie, and Kevin Zhang. 2025. Multi-Modal Large Language Model with RAG Strategies in Soccer Commentary Generation. In *WACV*. 6197–6206.
- [23] Zhe Li, Xiangfei Qiu, Peng Chen, Yihang Wang, Hanyin Cheng, Yang Shu, Jilin Hu, Chenjuan Guo, Aoying Zhou, Qingsong Wen, et al. 2025. TSMF-Bench: A Comprehensive and Unified Benchmark of Foundation Models for Time Series Forecasting. In *SIGKDD*.
- [24] Bryan Lim, Sercan Ö Arık, Nicolas Loeff, and Tomas Pfister. 2021. Temporal fusion transformers for interpretable multi-horizon time series forecasting. 37, 4 (2021), 1748–1764.
- [25] Shengsheng Lin, Weiwei Lin, Wentai Wu, Haojun Chen, and Junjie Yang. 2024. SparseTSF: Modeling Long-term Time Series Forecasting with 1k Parameters. In *ICML*. 30211–30226.
- [26] Shengsheng Lin, Weiwei Lin, HU Xinyi, Wentai Wu, Ruichao Mo, and Haocheng Zhong. 2024. CycleNet: Enhancing Time Series Forecasting through Modeling Periodic Patterns. In *NeurIPS*.
- [27] Yan Lin, Jilin Hu, Shengnan Guo, Bin Yang, Christian S Jensen, Youfang Lin, and Huaiyu Wan. 2024. GenSTL: General Sparse Trajectory Learning via Autoregressive Generation of Feature Domains. *arXiv preprint arXiv:2402.07232* (2024).
- [28] Peiyuan Liu, Hang Guo, Tao Dai, Naiqi Li, Jigang Bao, Xudong Ren, Yong Jiang, and Shu-Tao Xia. 2025. CALF: Aligning LLMs for Time Series Forecasting via Cross-modal Fine-Tuning. *AAAI* 39, 18 (2025), 18915–18923.
- [29] Peiyuan Liu, Beiliang Wu, Yifan Hu, Naiqi Li, Tao Dai, Jigang Bao, and Shu-Tao Xia. 2025. TimeBridge: Non-Stationarity Matters for Long-term Time Series Forecasting. *ICML* (2025).
- [30] Xvyan Liu, Xiangfei Qiu, Xingjian Wu, Zhengyu Li, Chenjuan Guo, Jilin Hu, and Bin Yang. 2025. Rethinking Irregular Time Series Forecasting: A Simple yet Effective Baseline. *arXiv preprint arXiv:2505.11250* (2025).
- [31] Shilin Lu, Yanzhu Liu, and Adams Wai-Kin Kong. 2023. Tf-icon: Diffusion-based training-free cross-domain image composition. In *ICCV*. 2294–2305.
- [32] Shilin Lu, Zilan Wang, Leyang Li, Yanzhu Liu, and Adams Wai-Kin Kong. 2024. Mace: Mass concept erasure in diffusion models. In *CVPR*. 6430–6440.
- [33] Shilin Lu, Zihan Zhou, Jiayou Lu, Yuanzhi Zhu, and Adams Wai-Kin Kong. 2024. Robust watermarking using generative priors against image editing: From benchmarking to advances. *arXiv preprint arXiv:2410.18775* (2024).
- [34] Xiaoye Miao, Yangyang Wu, Jun Wang, Yunjun Gao, Xudong Mao, and Jianwei Yin. 2021. Generative semi-supervised learning for multivariate time series imputation. In *AAAI*, Vol. 35. 8983–8991.
- [35] Xian Mo, Jun Pang, and Zhiming Liu. 2022. THS-GWNN: a deep learning framework for temporal network link prediction. *Frontiers of Computer Science* 16, 2 (2022), 162304.
- [36] Yuqi Nie, Nam H. Nguyen, Phanwadee Sinthong, and Jayant Kalagnanam. 2023. A Time Series is Worth 64 Words: Long-term Forecasting with Transformers. In *ICLR*.
- [37] Kin G Olivares, Cristian Challu, Grzegorz Marcjasz, Rafał Weron, and Artur Dubrawski. 2023. Neural basis expansion analysis with exogenous variables: Forecasting electricity prices with NBEATSx. 39, 2 (2023), 884–900.
- [38] Boris N. Oreshkin, Dmitri Carpov, Nicolas Chapados, and Yoshua Bengio. 2020. N-BEATS: Neural basis expansion analysis for interpretable time series forecasting. In *ICLR*.
- [39] Adam Paszke, Sam Gross, Francisco Massa, Adam Lerer, James Bradbury, Gregory Chanan, Trevor Killeen, Zeming Lin, Natalia Gimelshein, Luca Antiga, Alban Desmaison, Andreas Köpf, Edward Z. Yang, Zachary DeVito, Martin Raison, Alykhan Tejani, Sasank Chilamkurthy, Benoit Steiner, Lu Fang, Junjie Bai, and Soumith Chintala. 2019. PyTorch: An Imperative Style, High-Performance Deep Learning Library. In *NeurIPS*. 8024–8035.
- [40] Xuecheng Qi, Huiqi Hu, Jinwei Guo, Chenchen Huang, Xuan Zhou, Ning Xu, Yu Fu, and Aoying Zhou. 2023. High-availability in-memory key-value store using RDMA and Optane DCPMM. *Frontiers of Computer Science* 17, 1 (2023), 171603.
- [41] Xiangfei Qiu, Hanyin Cheng, Xingjian Wu, Jilin Hu, and Chenjuan Guo. 2025. A Comprehensive Survey of Deep Learning for Multivariate Time Series Forecasting: A Channel Strategy Perspective. *arXiv preprint arXiv:2502.10721* (2025).
- [42] Xiangfei Qiu, Jilin Hu, Lekui Zhou, Xingjian Wu, Junyang Du, Buang Zhang, Chenjuan Guo, Aoying Zhou, Christian S. Jensen, Zhenli Sheng, and Bin Yang. 2024. TFB: Towards Comprehensive and Fair Benchmarking of Time Series Forecasting Methods. *Proc. VLDB Endow.* 17, 9 (2024), 2363–2377.
- [43] Xiangfei Qiu, Xiuwen Li, Ruiyang Pang, Zhicheng Pan, Xingjian Wu, Liu Yang, Jilin Hu, Yang Shu, Xuesong Lu, Chengcheng Yang, Chenjuan Guo, Aoying Zhou, Christian S. Jensen, and Bin Yang. 2025. EasyTime: Time Series Forecasting Made Easy. In *ICDE*.
- [44] Xiangfei Qiu, Zhe Li, Wanghui Qiu, Shiyang Hu, Lekui Zhou, Xingjian Wu, Zhengyu Li, Chenjuan Guo, Aoying Zhou, Zhenli Sheng, Jilin Hu, Christian S. Jensen, and Bin Yang. 2025. TAB: Unified Benchmarking of Time Series Anomaly Detection Methods. In *Proc. VLDB Endow.*
- [45] Xiangfei Qiu, Xingjian Wu, Yan Lin, Chenjuan Guo, Jilin Hu, and Bin Yang. 2025. Duet: Dual Clustering Enhanced Multivariate Time Series Forecasting. In *SIGKDD*. 1185–1196.
- [46] David Salinas, Valentin Flunkert, Jan Gasthaus, and Tim Januschowski. 2020. DeepAR: Probabilistic forecasting with autoregressive recurrent networks. *International journal of forecasting* 36, 3 (2020), 1181–1191.
- [47] Omer Berat Sezer, Mehmet Ugur Gudelek, and Ahmet Murat Özbayoglu. 2020. Financial time series forecasting with deep learning: A systematic literature review: 2005-2019. *Appl. Soft Comput.* 90 (2020), 106181.
- [48] Artyom Stitsyuk and Jaesik Choi. 2025. xPatch: Dual-Stream Time Series Forecasting with Exponential Seasonal-Trend Decomposition. In *AAAI*, Vol. 39. 20601–20609.
- [49] Chenchen Sun, Yan Ning, Derong Shen, and Tiezheng Nie. 2023. Graph Neural Network-Based Short-Term Load Forecasting with Temporal Convolution. *Data Science and Engineering* (2023), 1–20.
- [50] Kshitij Tayal, Arvind Renganathan, Xiaowei Jia, Vipin Kumar, and Dan Lu. 2024. ExoTST: Exogenous-Aware Temporal Sequence Transformer for Time Series

- Prediction. In *ICDM*. 857–862.
- [51] Luan Tran, Manh Nguyen, and Cyrus Shahabi. 2019. Representation learning for early sepsis prediction. In *2019 Computing in Cardiology (CinC)*. 1–4.
- [52] Stylianos I Vagropoulos, GI Chouliaras, Evaggelos G Kardakos, Christos K Simoglou, and Anastasios G Bakirtzis. 2016. Comparison of SARIMAX, SARIMA, modified SARIMA and ANN-based models for short-term PV generation forecasting. In *ENERGYCON*. 1–6.
- [53] Feng Wan, Linsen Li, Ke Wang, Lu Chen, Yunjun Gao, Weihao Jiang, and Shiliang Pu. 2022. MTPRE: a multi-scale spatial-temporal model for travel time prediction. In *SIGSPATIAL*. 1–10.
- [54] Jiaqi Wang, Tianyi Li, Anni Wang, Xiaoze Liu, Lu Chen, Jie Chen, Jianye Liu, Junyang Wu, Feifei Li, and Yunjun Gao. 2023. Real-time Workload Pattern Analysis for Large-scale Cloud Databases. *arXiv preprint arXiv:2307.02626* (2023).
- [55] Ruoyu Wang, Yangfan He, Tengjiao Sun, Xiang Li, and Tianyu Shi. 2025. UniT-MGE: Uniform Text-Motion Generation and Editing Model via Diffusion. In *WACV*. 6104–6114.
- [56] Yuxuan Wang, Haixu Wu, Jiayang Dong, Guo Qin, Haoran Zhang, Yong Liu, Yunzhong Qiu, Jianmin Wang, and Mingsheng Long. 2024. Timexer: Empowering transformers for time series forecasting with exogenous variables. In *NeurIPS*, Vol. 37. 469–498.
- [57] Kaimin Wei, Tianqi Li, Feiran Huang, Jinpeng Chen, and Zefan He. 2022. Cancer classification with data augmentation based on generative adversarial networks. *Frontiers of Computer Science* 16 (2022), 1–11.
- [58] Billy M Williams. 2001. Multivariate vehicular traffic flow prediction: Evaluation of ARIMAX modeling. 1776, 1 (2001), 194–200.
- [59] Haixu Wu, Jiehui Xu, Jianmin Wang, and Mingsheng Long. 2021. Autoformer: Decomposition Transformers with Auto-Correlation for Long-Term Series Forecasting. In *NeurIPS*. 22419–22430.
- [60] Xingjian Wu, Xiangfei Qiu, Hongfan Gao, Jilin Hu, Bin Yang, and Chenjuan Guo. 2025. K^2 VAE: A Koopman-Kalman Enhanced Variational AutoEncoder for Probabilistic Time Series Forecasting. In *ICML*.
- [61] Xingjian Wu, Xiangfei Qiu, Zhengyu Li, Yihang Wang, Jilin Hu, Chenjuan Guo, Hui Xiong, and Bin Yang. 2025. CATCH: Channel-Aware multivariate Time Series Anomaly Detection via Frequency Patching. In *ICLR*.
- [62] Xinle Wu, Xingjian Wu, Bin Yang, Lekui Zhou, Chenjuan Guo, Xiangfei Qiu, Jilin Hu, Zhenli Sheng, and Christian S. Jensen. 2024. AutoCTS++: zero-shot joint neural architecture and hyperparameter search for correlated time series forecasting. *VLDB J.* 33, 5 (2024), 1743–1770.
- [63] Ronghui Xu, Meng Chen, Yongshun Gong, Yang Liu, Xiaohui Yu, and Liqiang Nie. 2023. TME: Tree-guided Multi-task Embedding Learning towards Semantic Venue Annotation. *ACM Transactions on Information Systems* 41, 4 (2023), 1–24.
- [64] Chen Yang, Yangfan He, Aaron Xuxiang Tian, Dong Chen, Jianhui Wang, Tianyu Shi, Arsalan Heydarian, and Pei Liu. 2024. Wcdt: World-centric diffusion transformer for traffic scene generation. *arXiv preprint arXiv:2404.02082* (2024).
- [65] Ailing Zeng, Muxi Chen, Lei Zhang, and Qiang Xu. 2023. Are transformers effective for time series forecasting?. In *AAAI*, Vol. 37. 11121–11128.
- [66] Haoyi Zhou, Shanghang Zhang, Jieqi Peng, Shuai Zhang, Jianxin Li, Hui Xiong, and Wancai Zhang. 2021. Informer: Beyond efficient transformer for long sequence time-series forecasting. In *AAAI*, Vol. 35. 11106–11115.
- [67] Pengfei Zhou, Yunlong Liu, Junli Liang, Qi Song, and Xiangyang Li. 2025. CrossLinear: Plug-and-Play Cross-Correlation Embedding for Time Series Forecasting with Exogenous Variables. In *SIGKDD*.
- [68] Tian Zhou, Ziqing Ma, Qingsong Wen, Xue Wang, Liang Sun, and Rong Jin. 2022. Fedformer: Frequency enhanced decomposed transformer for long-term series forecasting. In *ICML*. 27268–27286.
- [69] Yiyang Zhou, Yangfan He, Yaofeng Su, Siwei Han, Joel Jang, Gedas Bertasius, Mohit Bansal, and Huaxiu Yao. 2025. ReAgent-V: A Reward-Driven Multi-Agent Framework for Video Understanding. *arXiv preprint arXiv:2506.01300* (2025).

A Experimental Details

A.1 Datasets

We perform experiments on eight common multivariate forecasting datasets: (1) **ETT** includes four subsets: ETTh1 and ETTh2 provide hourly recordings, while ETTm1 and ETTm2 contain data collected every 15 minutes. The endogenous variable is oil temperature, and the six power load features are used as exogenous variables. (2) **Weather** consists of 21 meteorological variables recorded every 10 minutes during 2020 at the Weather Station of the Max Planck Biogeochemistry Institute. The endogenous variable is the Wet Bulb factor, while the remaining indicators are used as exogenous variables. (3) **Electricity** consists of hourly electricity consumption data from 321 clients. The electricity consumption of the last client is the endogenous variable, and the consumption data from the other clients are used as exogenous variables. (4) **Exchange** collects daily exchange rates of eight countries from 1990 to 2016. The exchange rate of the last country is the endogenous variable, and the exchange rates of the others serve as exogenous variables. (5) **Traffic** records hourly road occupancy rates from 862 sensors on Bay Area freeways. We use the last sensor as the endogenous variable and others as exogenous variables.

we conduct experiments on 12 real-world datasets that satisfy the TSF-X conditions, including 5 EPF [19, 56] datasets and 7 datasets we sourced ourselves: (1) **NP** records Nord Pool market with hourly electricity price as the endogenous variable, and grid load and wind power forecast as exogenous features. (2) **PJM** records the Pennsylvania–New Jersey–Maryland Interconnection market, with zonal electricity price in the Commonwealth Edison (COMED) area as the endogenous variable, and corresponding system load and COMED load forecasts as exogenous variables. (3) **BE** records Belgium’s electricity market, with hourly electricity price as the endogenous variable, and load forecast in Belgium together with generation forecast from France as exogenous variables. (4) **FR** records the electricity market in France, where the electricity price is the endogenous variable, and generation and load forecasts are used as exogenous variables. (5) **DE** records the German electricity market, with hourly electricity price as the endogenous variable, and zonal load forecast in the Amprion area along with wind and solar generation forecasts as exogenous variables.

In addition to the 5 EPF [19, 56] datasets, we also conduct experiments on 7 datasets that we sourced ourselves, which satisfy the TSF-X conditions. (1) **Energy** provides hourly power generation data collected from the national grid operator in Chile, encompassing multiple energy sources such as battery storage, wind, hydro, solar, and thermoelectric generation. The thermoelectric generation is used as the endogenous variable, while the remaining energy types serve as exogenous variables. (2 & 3) **Colbun and Rapel** represent two daily-resolution hydropower datasets from Chile, containing water level, precipitation, and tributary inflow measurements for the Colbún and Rapel reservoirs. The water level is treated as the endogenous variable, while precipitation and inflow are used as exogenous variables. (4-7) **Sdwpf** comprises four wind power generation datasets collected from two turbines in the Longyuan wind farm, including Sdwpfm1 and Sdwpfm2 with hourly resolution, and Sdwpfh1 and Sdwpfh2 with half-hourly resolution. The active power output (Patv) is used as the endogenous variable. The exogenous variables include external weather environment

data collected from the ERA5 [13], such as temperature, surface pressure, relative humidity, wind speed, wind direction, and total precipitation.

A.2 Implementation Details

1) To keep consistent with previous works, we adopt Mean Squared Error (mse) and Mean Absolute Error (mae) as evaluation metrics. 2) We consider four forecasting horizon F : 96, 192, 336, and 720 for the eight common multivariate forecasting datasets. The look-back windows is fixed at 96 for all the baselines. 3) For the 12 real-world datasets that satisfy the TSF-X conditions, we conduct both long-term and short-term prediction experiments. For the Colbun and Rapel datasets, the short-term prediction uses a lookback window of 60 with a prediction horizon of 10, while the long-term prediction uses a lookback window of 180 with a prediction horizon of 30. For the other datasets, the short-term prediction uses a lookback window of 168 with a prediction horizon of 24, and the long-term prediction uses a lookback window of 720 with a prediction horizon of 360. 4) We utilize the TFB [42] code repository for unified evaluation, with all baseline results also derived from TFB. Following the settings in TFB [42] and TSFM-Bench [23], we do not apply the “Drop Last” trick to ensure a fair comparison. 5) All experiments of DAG are conducted using PyTorch [39] in Python 3.8 and executed on an NVIDIA Tesla-A800 GPU. The training process is guided by the L1 loss function and employs the ADAM optimizer. The initial batch size is set to 64, with the flexibility to halve it (down to a minimum of 8) in case of an Out-Of-Memory (OOM) issue.

A.3 MLP Fusion Approach

For methods that do not support future covariates, we adapt them to incorporate future exogenous variables using an MLP fusion approach—see Algorithm 1. Note that, for fairness, all methods in our experiments use historical endogenous variables, historical exogenous variables, and future exogenous variables.

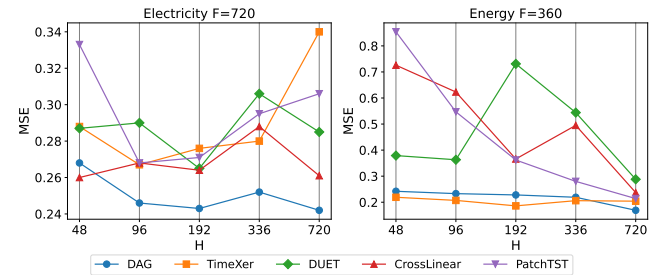


Figure 5: Forecasting performance (MSE) with varying look-back windows on 2 datasets: Electricity and Energy. The look-back windows are selected to be $H = 48, 96, 192, 336$ and 720 , and the forecasting horizons are $F = 720$ and 360 .

B Experimental Results

B.1 Full Results

Full results on multivariate datasets with TSF-X task, where the inputs are $(X^{\text{endo}}, X^{\text{exo}}, \text{ and } Y^{\text{exo}})$ are provided in Table 6.

Table 5: Statistics of datasets. Ex. and En. are abbreviations for the Exogenous variable and Endogenous variable, respectively.

Dataset	#Num	Ex. Descriptions	En. Descriptions	Sampling Frequency	Lengths	Split
ETTh	6	Power Load Feature	Oil Temperature	1 Hour	14,400	6:2:2
ETM	6	Power Load Feature	Oil Temperature	15 Minutes	57,600	6:2:2
Weather	20	Climate Feature	CO2-Concentration	10 Minutes	52,696	7:1:2
Exchange	7	Exchange Rate	Exchange Rate	1 Day	7,588	7:1:2
Electricity	320	Electricity Consumption	Electricity Consumption	1 Hour	26,304	7:1:2
Traffic	861	Road Occupancy Rates	Road Occupancy Rates	1 Hour	17,544	7:1:2
NP	2	Grid Load, Wind Power	Nord Pool Electricity Price	1 Hour	52,416	7:1:2
PJM	2	System Load, SyZonal COMED load	Pennsylvania-New Jersey-Maryland Electricity Price	1 Hour	52,416	7:1:2
BE	2	Generation, System Load	Belgium's Electricity Price	1 Hour	52,416	7:1:2
FR	2	Generation, System Load	France's Electricity Price	1 Hour	52,416	7:1:2
DE	2	Wind power, Ampirion zonal load	German's Electricity Price	1 Hour	52,416	7:1:2
Energy	5	Battery, Geothermal, Hydroelectric, Solar, Wind	Thermoelectric	1 Hour	13,064	7:1:2
Colbún	2	Precipitation, Tributary Inflow	Water Level	1 Day	2,958	7:1:2
Rapel	2	Precipitation, Tributary Inflow	Water Level	1 Day	3,366	7:1:2
Sdwpfh	6	Climate Feature	Active Power	1 Hour	1,4641	7:1:2
Sdwpfm	6	Climate Feature	Active Power	30 Minutes	2,9281	7:1:2

Algorithm 1 MLP Fusion Approach

Input: model parameters θ_{Model} , MLP parameters θ_{MLP} ; learning rate η ; iterations N ; training dataset D ; historical endogenous variables X^{endo} ; historical exogenous variables X^{exo} ; future exogenous variables Y^{exo}

Output: prediction \hat{Y}^{endo}

```

1: Training Phase:
2: For  $i = 1$  to  $N$  do
3:   For  $(X_{\text{train}}^{\text{endo}}, X_{\text{train}}^{\text{exo}}, Y_{\text{train}}^{\text{endo}}, Y_{\text{train}}^{\text{exo}})$  in  $D$ 
4:      $z \leftarrow \theta_{\text{Model}}(X_{\text{train}}^{\text{endo}}, X_{\text{train}}^{\text{exo}})$ 
5:      $\hat{Y}^{\text{endo}} \leftarrow \theta_{\text{MLP}}(\text{Concat}(z, Y_{\text{train}}^{\text{exo}}))$ 
6:      $\mathcal{L} \leftarrow \text{Loss}(\hat{Y}^{\text{endo}}, Y_{\text{train}}^{\text{endo}})$ 
7:      $\theta_{\text{Model}} \leftarrow \theta_{\text{Model}} - \eta \frac{\partial \mathcal{L}}{\partial \theta_{\text{Model}}}$ ,  $\theta_{\text{MLP}} \leftarrow \theta_{\text{MLP}} - \eta \frac{\partial \mathcal{L}}{\partial \theta_{\text{MLP}}}$ 
8:   EndFor
9: EndFor
10: Inference Phase:
11:  $z \leftarrow \theta_{\text{Model}}(X^{\text{endo}}, X^{\text{exo}})$ 
12:  $\hat{Y}^{\text{endo}} \leftarrow \theta_{\text{MLP}}(\text{Concat}(z, Y^{\text{exo}}))$ 
13: return  $\hat{Y}^{\text{endo}}$ 

```

B.2 Increasing Look-back Window

In time series forecasting tasks, the size of the look-back window determines how much historical information the model receives. We select models with better predictive performance from the main experiments as baselines. We configure different look-back window to evaluate the effectiveness of DAG and visualize the prediction results for look-back window H of 48, 96, 192, 336, 720, and the forecasting horizons are $F = 720, 360$. From Figure 5, DAG consistently outperforms the baselines on the Electricity, and Energy. As the look-back window increases, the prediction metrics of DAG continue to decrease, indicating that it is capable of modeling longer sequences.

Table 6: Full results on multivariate datasets with TSF-X task, where the inputs are (X^{endo} , X^{exo} , and Y^{exo}). The forecasting horizons $F \in \{96, 192, 336, 720\}$ and look-back window is set to 96. Avg means the average results from all four forecasting horizons. **Red: the best, **Blue**: the 2nd best.**

Models	Metrics	DAG (ours)		TimeXer		TFT		TiDE		DUET		CrossLinear		Amplifier		TimeKAN		xPatch		PatchTST		DLinear	
		mse	mae	mse	mae	mse	mae	mse	mae	mse	mae	mse	mae	mse	mae								
ETTh1	96	0.054	0.176	0.056	<u>0.179</u>	0.081	0.214	<u>0.056</u>	0.179	0.163	0.338	0.152	0.321	0.160	0.332	0.118	0.273	0.136	0.305	0.216	0.403	0.176	0.351
	192	0.072	<u>0.208</u>	<u>0.073</u>	0.207	0.073	0.213	0.075	0.210	0.206	0.382	0.199	0.374	0.134	0.290	0.166	0.330	0.150	0.311	0.174	0.336	0.227	0.399
	336	0.079	0.219	<u>0.089</u>	<u>0.234</u>	0.099	0.246	0.090	0.236	0.248	0.419	0.218	0.383	0.162	0.325	0.140	0.295	0.133	0.291	0.253	0.429	0.187	0.355
	720	0.079	0.221	0.104	0.254	0.124	0.282	<u>0.096</u>	<u>0.244</u>	0.283	0.446	0.295	0.475	0.263	0.429	0.284	0.440	0.239	0.406	0.302	0.462	0.350	0.511
	Avg	0.071	0.206	0.081	0.219	0.094	0.239	<u>0.079</u>	<u>0.217</u>	0.225	0.396	0.216	0.388	0.180	0.344	0.177	0.335	0.165	0.328	0.236	0.407	0.235	0.404
ETTh2	96	0.127	<u>0.273</u>	0.141	0.289	0.217	0.364	0.127	0.271	<u>0.121</u>	0.275	0.135	0.289	0.119	0.275	0.122	0.278	0.191	0.352	0.134	0.293	0.189	0.343
	192	0.177	0.327	0.194	0.346	0.256	0.405	0.179	0.327	0.234	0.391	0.154	0.323	0.200	0.356	0.186	0.354	0.142	<u>0.305</u>	0.158	0.326	<u>0.142</u>	0.303
	336	0.215	0.369	0.226	0.380	0.287	0.435	0.223	0.375	0.228	0.379	<u>0.179</u>	0.343	0.209	0.367	0.181	0.342	0.185	0.349	0.172	0.338	0.180	<u>0.339</u>
	720	<u>0.214</u>	<u>0.370</u>	0.234	0.385	0.283	0.431	0.253	0.405	0.209	0.365	0.319	0.463	0.348	0.488	0.337	0.473	0.223	0.385	0.337	0.475	0.257	0.405
	Avg	0.183	0.335	0.199	0.350	0.261	0.409	0.195	<u>0.344</u>	0.198	0.352	0.197	0.354	0.219	0.372	0.207	0.362	<u>0.185</u>	0.348	0.200	0.358	0.192	0.348
ETTm1	96	0.029	0.127	0.030	<u>0.129</u>	<u>0.030</u>	0.131	0.030	0.130	0.063	0.204	0.087	0.247	0.092	0.252	0.067	0.205	0.055	0.188	0.092	0.253	0.059	0.188
	192	0.044	0.159	0.044	<u>0.161</u>	0.048	0.168	0.049	0.168	0.217	0.413	0.164	0.351	0.177	0.359	0.156	0.331	0.128	0.300	0.132	0.304	0.189	0.378
	336	0.057	0.184	<u>0.060</u>	<u>0.189</u>	0.068	0.200	0.069	0.203	0.252	0.446	0.239	0.426	0.247	0.435	0.191	0.363	0.155	0.333	0.255	0.440	0.220	0.371
	720	0.079	<u>0.216</u>	0.082	0.222	0.095	0.240	0.073	0.211	0.265	0.436	0.286	0.462	0.252	0.424	0.261	0.428	0.247	0.425	0.251	0.434	0.282	0.458
	Avg	0.052	0.172	<u>0.054</u>	<u>0.175</u>	0.060	0.185	0.055	0.178	0.199	0.375	0.194	0.372	0.192	0.367	0.169	0.332	0.146	0.312	0.183	0.358	0.187	0.349
ETTm2	96	0.063	0.183	0.072	0.195	0.117	0.253	<u>0.070</u>	<u>0.190</u>	0.107	0.260	0.156	0.332	0.175	0.353	0.146	0.309	0.151	0.320	0.173	0.351	0.113	0.264
	192	<u>0.098</u>	0.230	0.110	0.249	0.179	0.324	0.101	0.235	0.200	0.366	0.203	0.366	0.179	0.339	0.139	0.293	0.096	<u>0.235</u>	0.142	0.295	0.156	0.307
	336	0.127	0.270	0.139	0.284	0.206	0.356	<u>0.128</u>	<u>0.272</u>	0.136	0.292	0.136	0.292	0.139	0.294	0.182	0.338	0.141	0.291	0.151	0.311	0.137	0.293
	720	0.179	0.328	0.190	0.340	0.271	0.417	0.179	0.328	0.147	0.310	0.156	0.316	0.175	0.332	0.169	0.332	0.204	0.362	0.164	0.326	<u>0.152</u>	<u>0.310</u>
	Avg	0.117	0.253	0.128	0.267	0.193	0.338	<u>0.119</u>	<u>0.256</u>	0.148	0.307	0.163	0.326	0.167	0.330	0.159	0.318	0.148	0.302	0.157	0.321	0.139	0.294
Weather	96	0.001	0.023	0.001	0.023	0.001	0.028	0.001	0.026	0.002	0.028	0.012	0.093	0.008	0.074	0.008	0.072	0.001	0.027	0.006	0.062	0.008	0.076
	192	0.001	0.022	0.001	0.026	0.002	0.030	0.001	0.028	0.002	0.030	0.005	0.056	0.008	0.073	0.009	0.078	0.001	<u>0.024</u>	0.008	0.073	0.006	0.065
	336	0.002	0.028	0.001	<u>0.027</u>	0.002	0.030	0.002	0.031	0.001	0.025	0.009	0.080	0.008	0.071	0.009	0.074	0.002	0.029	0.011	0.087	0.010	0.081
	720	0.002	0.030	0.002	<u>0.032</u>	0.002	0.035	0.002	0.036	0.002	0.033	0.007	0.067	0.019	0.113	0.003	0.045	0.002	0.037	0.012	0.084	0.014	0.098
	Avg	0.002	0.026	0.001	<u>0.027</u>	0.002	0.031	0.002	0.030	<u>0.002</u>	0.029	0.008	0.074	0.011	0.083	0.007	0.067	0.002	0.029	0.009	0.076	0.010	0.080
Electricity	96	0.158	<u>0.298</u>	<u>0.160</u>	0.296	0.365	0.456	0.312	0.414	0.248	0.385	0.281	0.416	0.279	0.416	0.276	0.413	0.249	0.387	0.274	0.406	0.301	0.433
	192	0.156	0.295	<u>0.186</u>	<u>0.320</u>	0.339	0.448	0.274	0.391	0.290	0.421	0.248	0.384	0.296	0.427	0.309	0.435	0.258	0.397	0.264	0.399	0.303	0.427
	336	0.217	<u>0.353</u>	<u>0.218</u>	0.346	0.367	0.471	0.313	0.417	0.295	0.426	0.260	0.396	0.278	0.414	0.292	0.419	0.296	0.425	0.271	0.408	0.253	0.396
	720	0.246	0.370	0.267	<u>0.386</u>	0.429	0.510	0.353	0.445	0.290	0.414	0.268	0.401	<u>0.255</u>	0.396	0.327	0.448	0.256	0.392	0.268	0.402	0.296	0.422
	Avg	0.194	0.329	<u>0.208</u>	<u>0.337</u>	0.375	0.471	0.313	0.417	0.281	0.411	0.264	0.399	0.277	0.413	0.301	0.429	0.265	0.400	0.269	0.404	0.288	0.420
Traffic	96	0.119	0.187	<u>0.135</u>	0.233	0.139	<u>0.221</u>	0.149	0.251	0.247	0.316	0.261	0.322	0.174	0.240	0.221	0.292	0.244	0.305	0.241	0.307	0.185	0.258
	192	<u>0.121</u>	0.191	0.135	0.230	0.116	<u>0.212</u>	0.149	0.246	0.240	0.297	0.232	0.289	0.214	0.276	0.181	0.254	0.220	0.292	0.246	0.305	0.240	0.306
	336	0.125	0.200	0.143	0.237	<u>0.134</u>	<u>0.228</u>	0.150	0.251	0.310	0.356	0.223	0.280	0.188	0.318	0.210	0.283	0.211	0.278	0.215	0.280	0.241	0.313
	720	<u>0.152</u>	<u>0.232</u>	0.156	0.250	0.138	0.220	0.169	0.271	0.253	0.318	0.213	0.272	0.201	0.271	0.231	0.310	0.210	0.273	0.229	0.286	0.183	0.247
	Avg	0.129	0.203	0.142	0.238	<u>0.132</u>	<u>0.220</u>	0.154	0.255	0.263	0.322	0.232	0.291	0.194	0.276	0.211	0.285	0.221	0.287	0.233	0.295	0.212	0.281
Exchange	96	0.087	0.229	0.109	0.245	0.105	0.258	<u>0.096</u>	<u>0.230</u>	0.291	0.484	0.234	0.425	0.136	0.316	0.297	0.487	0.220	0.397	0.370	0.554	0.113	0.283
	192	0.147	0.298	0.197	0.350	0.258	0.393	0.205	0.340	0.236	0.421	0.231	0.430	0.186	0.360	0.300	0.461	<u>0.153</u>	<u>0.334</u>	0.427	0.590	0.363	0.525
	336	0.274	0.413	0.331	<u>0.444</u>	0.422	0.524	0.453	0.519	<u>0.309</u>	0.496	0.394	0.563	0.412	0.562	0.716	0.752	0.484	0.610	0.558	0.687	0.427	0.576
	720	0.338	<u>0.470</u>	0.362	0.482	0.552	0.577	0.419	0.502	0.244	0.419	0.390	0.558	0.459	0.614	0.387	0.559	<u>0.336</u>	0.511	0.503	0.640	0.550	0.655
	Avg	0.212	0.353	<u>0.250</u>	<u>0.380</u>	0.334	0.438	0.293	0.398	0.270	0.455	0.312	0.494	0.298	0.463	0.425	0.565	0.298	0.463	0.464	0.618	0.363	0.510
1 st Count	28	28	<u>5</u>	<u>4</u>	2	1	1	2	<u>5</u>	<u>4</u>	0	0	1	0	0	0	0	2	0	1	1	0	1